

Detectability of Lung Nodules in Ultra-low Dose CT

SONJA JANSSEN, DANIEL OVERHOFF, MATTHIAS F. FROELICH,
STEFAN O. SCHOENBERG and NILS RATHMANN

*Department of Radiology and Nuclear Medicine, Medical Faculty Mannheim,
University of Heidelberg, Mannheim, Germany*

Abstract. *Background/Aim:* Investigation of the influence of different ultra-low dose computed tomography (ULDCT) protocols on the detection of solid and subsolid nodules in a phantom study. *Patients and Methods:* A chest phantom with pulmonary nodules was scanned with different CT protocols ranging from ultra-low dose settings with spectral shaping to a standard low dose lung cancer screening protocol. Image analysis was performed with different reconstruction algorithms and dedicated computer aided detection (CAD), which was compared to manual readout. *Results:* The highest sensitivity rates (83%) were achieved for the 90 mAs and 120 mAs protocols when reconstructed with ADMIRE 3 or 5 and manual readout. The only statistically significant difference was found for subsolid nodules with preference of manual readout compared to CAD ($p < 0.05$). Dose levels for the mAs settings ranged from 0.029 to 0.2 mSv. *Conclusion:* Reliable detectability rates for solid nodules were achieved; CAD software did not prove reliable for subsolid nodules.

A 20% reduction in lung cancer mortality can be achieved when screening with low-dose computed tomography (LDCT), compared with chest radiography (1). These results of the National Lung Screening trial led to an increasing acceptance of chest LDCT and computer-aided detection (CAD) software for screening (2). Recent efforts and recommendations have focused on who to screen, when to screen, and which are the best qualitative and quantitative parameters to detect and monitor malignancy (2, 3). In lung cancer screenings, the ALARA principle seems even more important. Thus, it is necessary to assess the accuracy of ultra-low dose scan

Correspondence to: Nils Rathmann, Department of Radiology and Nuclear Medicine, Medical Faculty Mannheim, University of Heidelberg, Theodor-Kutzer-Ufer 1-3, 68167 Mannheim, Germany. Tel: +49 6213832067, e-mail: nils.rathmann@umm.de

Key Words: Computed tomography, iterative reconstruction, pulmonary nodules, ultra-low dose, detectability, computer-aided detection, solid, subsolid.

protocols to reliably detect and measure pulmonary nodules. To reduce noise that accompanies low-dose CT protocols, the use of iterative reconstruction algorithms has become standard. However, iterative reconstruction algorithms have been shown to influence lung nodule detectability rates of manual readers and CAD software (4, 5).

Although studies tend to focus on solid nodules (6), subsolid nodules are also of high interest, since subsolid nodules are known to grow slowly and are more often malignant than solid nodules (7). In this context the aim of this study was to compare detectability of solid and subsolid lung nodules on ULDCT 100Sn kVp protocol at different tube current settings and levels of 3rd generation iterative reconstruction to a standard low-dose CT lung cancer screening protocol with and without CAD software.

Patients and Methods

This prospective phantom study was performed according to standards of the Health Insurance Portability and Accountability Act (HIPAA) and the Declaration of Helsinki. Institutional review board approval was dispensed due to the phantom character of the study.

Phantom. An anthropomorphic chest phantom (Lungman, Kyoto Kagaku, Tokyo, Japan) was used with artificial lung and pulmonary vessels (8). Fifteen artificial spherical pulmonary nodules were distributed within the phantom lungs. The nodules had different diameters of 5, 8, 10, and 12 mm (volume of 65, 268, 523, and 904 mm³), and three different CT densities of -800, -630 and +100 Hounsfield Units (HU). The specifications of the phantom and the nodules have been described in detail by Xie *et al.* (9).

Data acquisition. A 3rd generation dual-source CT system (2×192 slices; Somatom Force, Siemens Healthineers, Forchheim, Germany) was used for data acquisition. The ultra-low dose protocol had the following parameters: tube voltage 100 kVp with tin filter (100 kVp Sn) with tube current levels of 120 mAs, 90 mAs, 60 mAs and 30 mAs, pitch 1.2, rotation time 0.25 s, detector collimation 192×0.6 mm, slice thickness 1.5 mm, increment 1.0 mm, matrix size 512×512. For all mAs acquisitions, filtered back projection (FBP) reconstructions and 3rd generation advanced model-based iterative reconstruction (ADMIRE) were reconstructed with strengths of 1, 3, and 5. The physical background of ADMIRE

has been described in detail by Gordic *et al.* (6). The low-dose lung cancer screening protocol had the following parameters: tube voltage 120 kVp, tube current 20 mAs, pitch 1.5, slice thickness 1.5 mm, increment 1.0 mm, sharp lung kernel (B157) and window width with levels of 1,600 and -600.

Thirteen different nodule setups were used: 12 setups consisting of 6 nodules and one consisting of 3 nodules for blinding the reader. Each of the 13 nodule setups was scanned with the ultra-low dose protocol at the four mAs settings, and with the standard lung cancer screening protocol, resulting in 65 datasets. The 13 standard lung cancer screening protocol scans were reconstructed with FBP. The other 52, ultra-low dose CT scans were reconstructed with FBP, and ADMIRE 1, 3, and 5 resulting in 208 datasets. Thus, in total, 221 datasets were analyzed.

Image analysis. All datasets were analyzed by the LungCAD software (SyngoCT, CAD, VA 20, Siemens Healthineers) and by an experienced thoracic radiologist with 10 years of experience. A radiologist with 6 years of experience cross-read both analyses to determine the number of correctly detected solid and subsolid nodules, and possible false positives. Differences between detectability of solid and subsolid nodules between the different scan protocols were investigated. Readout was performed on the basis of B70 lung reconstruction kernel with possible maximum intensity projection of 5 to 6 slice packs and individual adjustment of window width and window center.

Statistical analysis. Statistical analyses were carried out in R Statistics (version 3.6.1, R Core Team, Vienna, Austria). For group comparisons, Fisher's exact test applied to categorical variables and the Mann-Whitney *U*-test was applied to ordinal or continuously scaled variables.

Sensitivity was determined as the number of true-positive nodules detected divided by the number of nodules distributed in the setup. The rate of true-positive nodules detected in every phantom setup was the number of nodules detected divided by the total number of structures detected in the setup. The rate of false-positive nodules was the number of structures detected in the phantom which were not true nodules divided by the total number of detected structures within the phantom. Diagnostic accuracies and respective standard errors were visualized using the package ggplot2. The level of significance was set to <0.05 .

Results

The sensitivity rate for all nodules combined manual readouts was superior to CAD analysis ($p < 0.0001$). Table I and Figure 1 display the sensitivity rates of the different protocols compared to one another. With manual readout, ADMIRE was not superior to FBP (max. mean sensitivity 83% vs. 84%). With CAD readout, ADMIRE 5 with the 90 mAs protocol was slightly superior compared to FBP with the 20 mAs protocol (sensitivity 52% vs. 41%). Manual analysis was not statistically significant superior to CAD analysis ($p > 0.05$) for the detection of solid lesions. For subsolid nodules the sensitivity rates for manual readout were statistically significantly higher than for CAD readout over all protocols ($p < 0.001$). Table I displays the results of the different protocols.

FBP with CAD readout and 20 mAs resulted in the highest false-positive rate for solid (1.07) and subsolid nodules (3.15) compared to the other readouts. Manual read-out did not show any false positive detections for solid nodules. The analysis of subsolid nodules showed that both methods, manual and CAD readout, resulted in false positive results, whereas for some reconstructions manual read-out was statically significantly better than CAD. Table II and Figure 2 display the false-positive detections. Table I and Table II also display the dose levels in mSv for each scan setting.

Discussion

One major goal of CAD analysis systems is to enhance the speed of screening a dataset and not missing any relevant finding. With the introduction of single-energy 100 kVp protocols with tin filtration (100Sn kVp) in 3rd generation dual-source CT systems for non-enhanced ULDCT scanning, radiation dose is markedly reduced due to spectral shaping (6).

Gordic *et al.* investigated the detectability of pulmonary nodules in a phantom study with two readers, and the use of the 100Sn kVp protocol in combination with 3rd generation iterative reconstruction algorithm with a standard dose level, a 1/10th dose level, and 1/20th dose level (6). They found the highest sensitivity rates ($>90\%$) for 100Sn kVp and ADMIRE 5 at the 1/10th and 1/20th dose levels. This study also showed that iterative reconstruction algorithms can result in high sensitivity rates for solid nodules using manual readout and CAD software. In this study, the ADMIRE protocols with manual readout in ULDCT at 100 kVp/tin filtration were similarly accurate in the detection of solid pulmonary nodules compared to a standard low-dose lung cancer screening protocol (120kV with 20mAs and FBP; sensitivity 89%), whereas a sensitivity rate higher than 80% was only found with a tube current of 90 mAs or higher. However, detectability rates of solid nodules with the CAD software could not be further increased compared to the rates of a manual readout.

The performance of ADMIRE protocols with manual readout in ULDCT were at least equally accurate in the detection of subsolid pulmonary nodules compared to a standard low-dose lung cancer screening protocol. CAD software also performed equally accurate in the detection of subsolid pulmonary nodules compared to a standard low-dose lung cancer screening protocol, but performed statistically significantly worse compared to manual readout (max 40% vs. min. 70%). Another study reported sensitivity rates for CAD systems between 23% to 38% (10). A draw back of the presented data seems to be that the dose was always higher with the ULDCT in comparison to the used low-dose lung cancer screening protocol with FBP and 20 mAs (Table I). However, the presented dose-levels were 0.2 mSv maximum and far below the dose-levels of "The National Lung Screening Trial" (NLST) protocol with 1.5 mSv using 120 kV and 40 to 80 mAs (1).

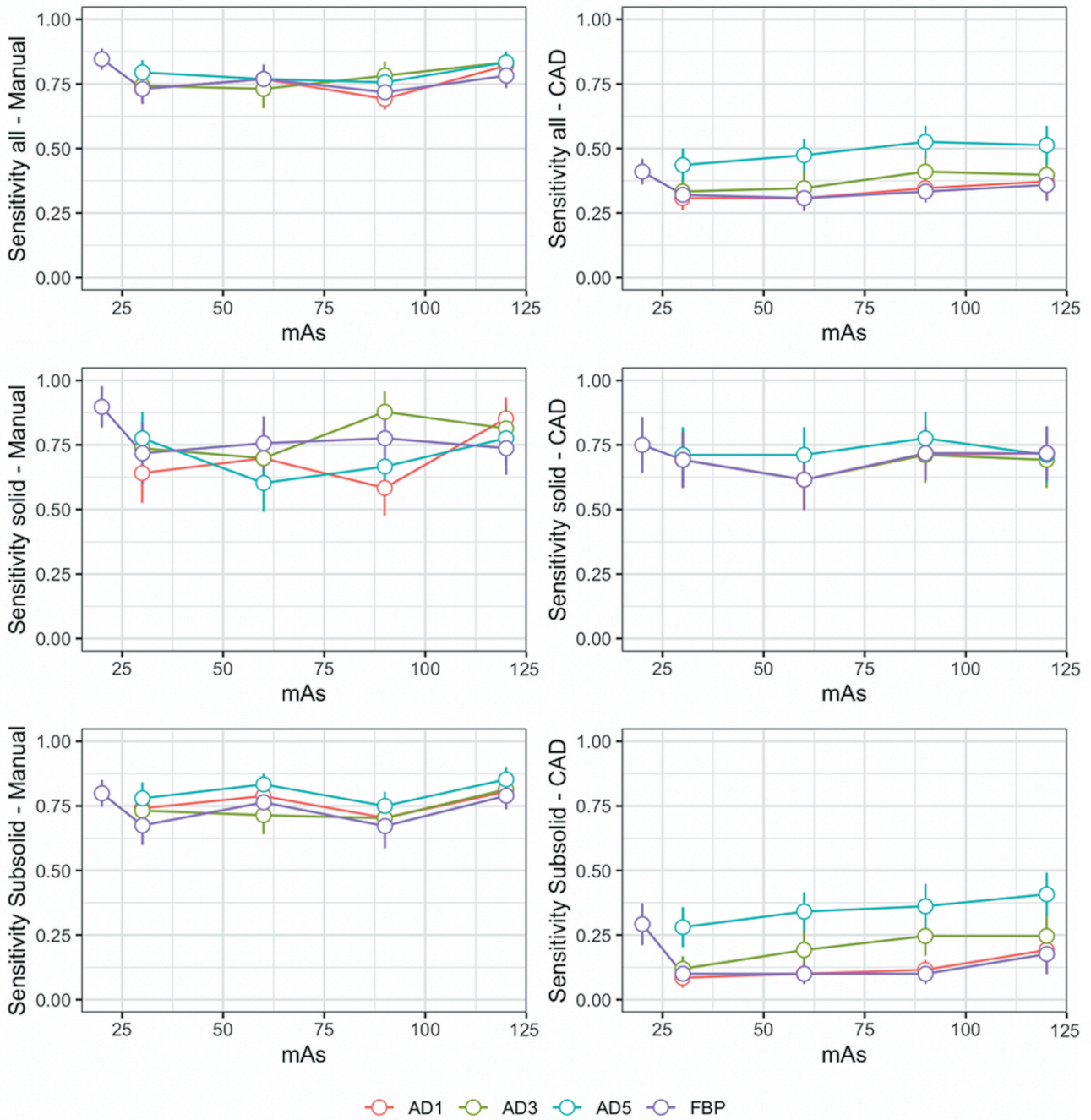


Figure 1. Mean sensitivity per mAs reconstruction for solid or subsolid nodules and overall. AD: ADMIRE, advanced model-based iterative reconstruction; FBP: filtered back projection; CAD: computer aided detection.

Leader *et al.* addressed another problem in the field of lung nodule detection: the smaller the nodules the more are missed (11). In this study using manual readout, no false-positive solid nodules were detected. In contrast, CAD analysis resulted for almost all setups in false-positive findings, including the standard lung cancer protocol

($p < 0.001$; Table II). For subsolid nodules both methods resulted in false-positive findings (Table II). These widespread results in sensitivity rates and the false-positive findings show that the use of CAD software needs to be handled with care. This suggests to not only use the CAD software for the detection of subsolid nodules.

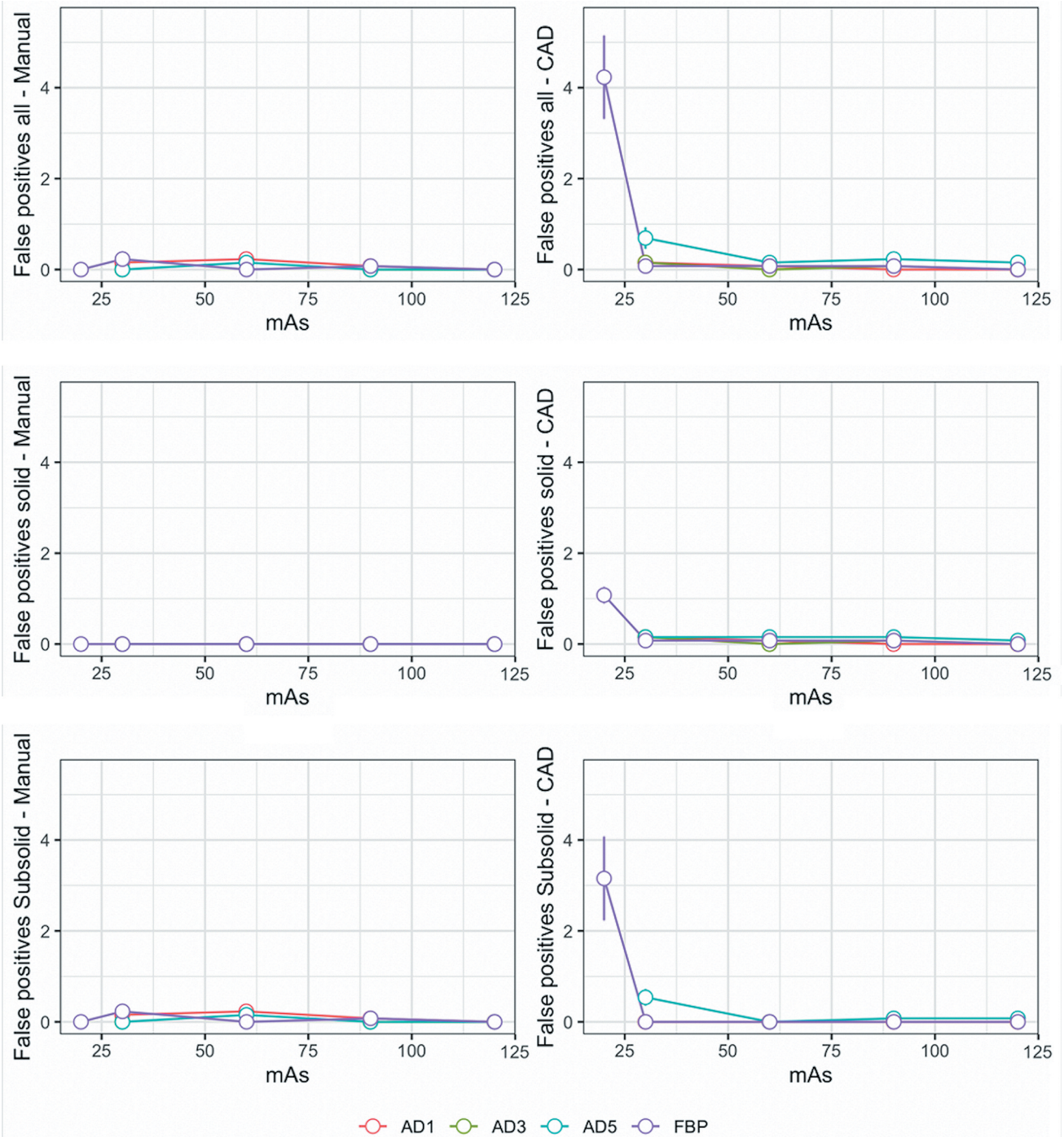


Figure 2. Mean number of false-positive findings per scanning setup for solid or subsolid nodules and overall. AD: ADMIRE, advanced model-based iterative reconstruction; FBP: filtered back projection; CAD: computer aided detection.

One technical limitation of the study was that the nodule distribution was only possible along to the bronchovascular bundle due to the structure of the phantom. Also, no lobulated or spiculated artificial nodules were used.

In conclusion iterative reconstruction algorithms and CAD software performed equally accurate in conventional low dose screening protocols and ultra-low dose 100 kVp/tin filtration protocols for detection of solid nodules

Table I. Comparison of the different scanning protocols. Mean sensitivity rates for the different scanning setups and comparison of manual to CAD readout for solid or subsolid nodules and overall, with standard deviation.

mAs	Recon	n	Sensitivity overall			Sensitivity solid nodules			Sensitivity subsolid nodules			Dose	
			Manual	CAD	p-Value	Manual	CAD	p-Value	Manual	CAD	p-Value	DLP	mSv
20	FBP	13	0.84 (0.14)	0.41 (0.17)	<0.001	0.89 (0.28)	0.75 (0.38)	0.19	0.79 (0.18)	0.29 (0.28)	<0.001	2.08	0.029
30	AD1	13	0.73 (0.17)	0.30 (0.16)	<0.001	0.64 (0.41)	0.69 (0.38)	0.76	0.74 (0.22)	0.08 (0.13)	<0.001	3.69	0.052
30	AD3	13	0.74 (0.14)	0.33 (0.18)	<0.001	0.73 (0.36)	0.69 (0.38)	0.77	0.73 (0.22)	0.11 (0.17)	<0.001	3.69	0.052
30	AD5	13	0.79 (0.16)	0.43 (0.23)	<0.001	0.77 (0.36)	0.71 (0.38)	0.67	0.77 (0.22)	0.28 (0.27)	<0.001	3.69	0.052
30	FBP	13	0.73 (0.21)	0.32 (0.15)	<0.001	0.71 (0.42)	0.69 (0.38)	0.89	0.67 (0.27)	0.1 (0.13)	<0.001	3.69	0.052
60	AD1	13	0.76 (0.14)	0.30 (0.17)	<0.001	0.69 (0.36)	0.61 (0.42)	0.57	0.78 (0.19)	0.1 (0.13)	<0.001	7.15	0.100
60	AD3	13	0.73 (0.26)	0.34 (0.24)	<0.001	0.69 (0.41)	0.61 (0.42)	0.62	0.71 (0.26)	0.19 (0.27)	<0.001	7.15	0.100
60	AD5	13	0.76 (0.14)	0.47 (0.22)	<0.001	0.60 (0.39)	0.71 (0.38)	0.50	0.83 (0.14)	0.34 (0.26)	<0.001	7.15	0.100
60	FBP	13	0.76 (0.19)	0.30 (0.17)	<0.001	0.75 (0.37)	0.61 (0.42)	0.35	0.76 (0.22)	0.1 (0.13)	<0.001	7.15	0.100
90	AD1	13	0.69 (0.14)	0.34 (0.15)	<0.001	0.58 (0.38)	0.71 (0.38)	0.40	0.70 (0.18)	0.11 (0.13)	<0.001	11.00	0.154
90	AD3	13	0.78 (0.19)	0.41 (0.22)	<0.001	0.87 (0.28)	0.71 (0.38)	0.14	0.70 (0.29)	0.24 (0.27)	<0.001	11.00	0.154
90	AD5	13	0.75 (0.17)	0.52 (0.22)	<0.001	0.66 (0.42)	0.77 (0.36)	0.52	0.75 (0.19)	0.36 (0.31)	<0.001	11.00	0.154
90	FBP	13	0.71 (0.22)	0.33 (0.15)	<0.001	0.77 (0.36)	0.71 (0.37)	0.70	0.67 (0.30)	0.1 (0.13)	<0.001	11.00	0.154
120	AD1	13	0.82 (0.14)	0.37 (0.21)	<0.001	0.85 (0.28)	0.71 (0.37)	0.24	0.80 (0.18)	0.19 (0.27)	<0.001	14.31	0.200
120	AD3	13	0.83 (0.13)	0.39 (0.25)	<0.001	0.81 (0.30)	0.69 (0.38)	0.31	0.81 (0.17)	0.24 (0.30)	<0.001	14.31	0.200
120	AD5	13	0.83 (0.15)	0.51 (0.26)	<0.001	0.77 (0.36)	0.71 (0.38)	0.67	0.85 (0.17)	0.40 (0.30)	<0.001	14.31	0.200
120	FBP	13	0.78 (0.17)	0.35 (0.22)	<0.001	0.73 (0.36)	0.71 (0.37)	0.90	0.78 (0.18)	0.17 (0.28)	<0.001	14.31	0.200

AD: ADMIRE, advanced model-based iterative reconstruction; FBP: filtered back projection; CAD: computer aided detection; DLP: dose length product.

Table II. Analysis of false positive rates for the different scanning protocols. Mean number of false positive findings per scanning setup for solid or subsolid nodules and overall, with standard deviation.

mAs	Recon	n	False positives overall			False positives solid nodules			False positives subsolid nodules			Dose	
			Manual	CAD	p-Value	Manual	CAD	p-Value	Manual	CAD	p-Value	DLP	mSv
20	FBP	13	0 (0)	4.23 (3.29)	<0.001	0 (0)	1.07 (0.64)	<0.001	0 (0)	3.15 (3.31)	<0.001	2.08	0.029
30	AD1	13	0.15 (0.55)	0.15 (0.37)	1.00	0 (0)	0.15 (0.37)	<0.001	0.15 (0.55)	0 (0)	0.49	3.69	0.052
30	AD3	13	0 (0)	0.15 (0.37)	<0.001	0 (0)	0.15 (0.37)	<0.001	0 (0)	0 (0)	-	3.69	0.052
30	AD5	13	0 (0)	0.69 (0.85)	<0.001	0 (0)	0.15 (0.37)	<0.001	0 (0)	0.53 (0.66)	<0.001	3.69	0.052
30	FBP	13	0.23 (0.59)	0.07 (0.27)	0.52	0 (0)	0.07 (0.27)	<0.001	0.23 (0.59)	0 (0)	0.33	3.69	0.052
60	AD1	13	0.23 (0.43)	0.07 (0.27)	0.38	0 (0)	0.07 (0.27)	<0.001	0.23 (0.43)	0 (0)	0.18	7.15	0.100
60	AD3	13	0.07 (0.27)	0 (0)	0.49	0 (0)	0 (0)	-	0.07 (0.27)	0 (0)	0.49	7.15	0.100
60	AD5	13	0.15 (0.37)	0.15 (0.37)	1.00	0 (0)	0.15 (0.37)	<0.001	0.15 (0.37)	0 (0)	0.30	7.15	0.100
60	FBP	13	0 (0)	0.07 (0.27)	<0.001	0 (0)	0.07 (0.27)	<0.001	0 (0)	0 (0)	-	7.15	0.100
90	AD1	13	0.07 (0.27)	0 (0)	0.49	0 (0)	0 (0)	-	0.07 (0.27)	0 (0)	0.49	11.00	0.154
90	AD3	13	0 (0)	0.07 (0.27)	<0.001	0 (0)	0.07 (0.27)	<0.001	0 (0)	0 (0)	-	11.00	0.154
90	AD5	13	0 (0)	0.23 (0.43)	<0.001	0 (0)	0.15 (0.37)	<0.001	0 (0)	0.07 (0.27)	<0.001	11.00	0.154
90	FBP	13	0.07 (0.27)	0.07 (0.27)	1.00	0 (0)	0.07 (0.27)	<0.001	0.07 (0.27)	0 (0)	0.49	11.00	0.154
120	AD1	13	0 (0)	0 (0)	-	0 (0)	0 (0)	-	0 (0)	0 (0)	-	14.31	0.200
120	AD3	13	0 (0)	0 (0)	-	0 (0)	0 (0)	-	0 (0)	0 (0)	-	14.31	0.200
120	AD5	13	0 (0)	0.15 (0.37)	<0.001	0 (0)	0.07 (0.27)	<0.001	0 (0)	0.07 (0.27)	<0.001	14.31	0.200
120	FBP	13	0 (0)	0 (0)	-	0 (0)	0 (0)	-	0 (0)	0 (0)	-	14.31	0.200

AD: ADMIRE, advanced model-based iterative reconstruction; FBP: filtered back projection; CAD: computer aided detection; DLP: dose length product.

in this study. However, CAD software was of limited use for the detection of subsolid nodules compared to manual readout.

Conflicts of Interest

The Authors state no relevant conflicts of interest associated with this work. The Department of Clinical Radiology and Nuclear Medicine has research agreements with Siemens Healthineers.

Authors' Contributions

SJ, DO, SOS and NR made substantial contributions to the conception and design of the study and acquisition of data. SJ, DO, MFF and NR analysed and interpreted the data. SJ, DO, MFF and NR drafted the article. SJ, DO, MFF, SOS and NR reviewed it critically for important intellectual content and gave final approval of the version to be published.

Acknowledgements

The Authors would like to express their sincere gratitude to Professor Rozemarijn Vliegthart from the Department of Radiology, University of Groningen - University Medical Center Groningen, the Netherlands, for providing us with the anthropomorphic chest phantom and for sharing all her precious knowledge and experience.

References

- National Lung Screening Trial Research Team., Aberle DR, Adams AM, Berg CD, Black WC, Clapp JD, Fagerstrom RM, Gareen IF, Gatsonis C, Marcus PM and Sicks JD: Reduced lung-cancer mortality with low-dose computed tomographic screening. *N Engl J Med* 365(5): 395-409, 2011. PMID: 21714641. DOI: 10.1056/NEJMoa1102873
- Wood DE, Kazerooni EA, Baum SL, Eapen GA, Ettinger DS, Hou L, Jackman DM, Klippenstein D, Kumar R, Lackner RP, Leard LE, Lennes IT, Leung ANC, Makani SS, Massion PP, Mazzone P, Merritt RE, Meyers BF, Midthun DE, Pipavath S, Pratt C, Reddy C, Reid ME, Rotter AJ, Sachs PB, Schabath MB, Schiebler ML, Tong BC, Travis WD, Wei B, Yang SC, Gregory KM and Hughes M: Lung cancer screening, version 3.2018, NCCN clinical practice guidelines in oncology. *J Natl Compr Canc Netw* 16(4): 412-441, 2018. PMID: 29632061. DOI: 10.6004/jnccn.2018.0020
- Oudkerk M, Devaraj A, Vliegthart R, Henzler T, Prosch H, Heussel CP, Bastarrika G, Sverzellati N, Mascalchi M, Delorme S, Baldwin DR, Callister ME, Becker N, Heuvelmans MA, Rzyman W, Infante MV, Pastorino U, Pedersen JH, Paci E, Duffy SW, de Koning H and Field JK: European position statement on lung cancer screening. *Lancet Oncol* 18(12): e754-e766, 2017. PMID: 29208441. DOI: 10.1016/S1470-2045(17)30861-6
- Den Harder AM, Willemink MJ, van Hamersvelt RW, Vonken EJ, Milles J, Schilham AM, Lammers JW, de Jong PA, Leiner T and Budde RP: Effect of radiation dose reduction and iterative reconstruction on computer-aided detection of pulmonary nodules: Intra-individual comparison. *Eur J Radiol* 85(2): 346-351, 2016. PMID: 26781139. DOI: 10.1016/j.ejrad.2015.12.003
- Botelho MP, Agrawal R, Gonzalez-Guindalini FD, Hart EM, Patel SK, Töre HG and Yaghamai V: Effect of radiation dose and iterative reconstruction on lung lesion conspicuity at MDCT: does one size fit all? *Eur J Radiol* 82(11): e726-e733, 2013. PMID: 23928232. DOI: 10.1016/j.ejrad.2013.07.011
- Gordic S, Morsbach F, Schmidt B, Allmendinger T, Flohr T, Husarik D, Baumüller S, Raupach R, Stolzmann P, Leschka S, Frauenfelder T and Alkadhi H: Ultralow-dose chest computed tomography for pulmonary nodule detection: first performance evaluation of single energy scanning with spectral shaping. *Invest Radiol* 49(7): 465-473, 2014. PMID: 24598443. DOI: 10.1097/RLI.0000000000000037
- Migliore M, Fornito M, Palazzolo M, Criscione A, Gangemi M, Borrata F, Vigneri P, Nardini M and Dunning J: Ground glass opacities management in the lung cancer screening era. *Ann Transl Med* 6(5): 90, 2018. PMID: 29666813. DOI: 10.21037/atm.2017.07.28
- Franck C, Snoeckx A, Spinhoven M, El Addouli H, Nicolay S, Van Hoyweghen A, Deak P and Zanca F: Pulmonary nodule detection in chest Ct using a deep learning-based reconstruction algorithm. *Radiat Prot Dosimetry*: ncab025, 2021. PMID: 33723584. DOI: 10.1093/rpd/ncab025
- Xie X, Willemink MJ, de Jong PA, van Ooijen PM, Oudkerk M, Vliegthart R and Greuter MJ: Small irregular pulmonary nodules in low-dose CT: observer detection sensitivity and volumetry accuracy. *AJR Am J Roentgenol* 202(3): W202-W209, 2014. PMID: 24555615. DOI: 10.2214/AJR.13.10830
- Larici AR, Amato M, Ordóñez P, Maggi F, Menchini L, Caulo A, Calandriello L, Vallati G, Giunta S, Crecco M and Bonomo L: Detection of noncalcified pulmonary nodules on low-dose MDCT: comparison of the sensitivity of two CAD systems by using a double reference standard. *Radiol Med* 117(6): 953-967, 2012. PMID: 22327922. DOI: 10.1007/s11547-012-0795-9
- Leader JK, Warfel TE, Fuhrman CR, Golla SK, Weissfeld JL, Avila RS, Turner WD and Zheng B: Pulmonary nodule detection with low-dose CT of the lung: agreement among radiologists. *AJR Am J Roentgenol* 185(4): 973-978, 2005. PMID: 16177418. DOI: 10.2214/AJR.04.1225

Received July 15, 2021

Revised August 27, 2021

Accepted August 30, 2021